PHYSICAL REVIEW E VOLUME 49, NUMBER 1 JANUARY 1994

Dynamics of dislocations in hexagonal patterns

M. I. Rabinovich* and L. S. Tsimring
Institute for Nonlinear Science, University of California, San Diego, California 92093-0402
(Received 24 August 1993)

The dynamics and interaction of dislocations of roll systems forming hexagonal patterns is studied numerically within a model of three resonantly coupled Newell-Whitehead-Segel equations. It is shown that an individual dislocation is driven away as a result of phase synchronization among roll patterns. Two dislocations with opposite topological charges belonging to different roll systems are attracted to each other and form a "penta-hepta" defect on the background of the perfect hexagonal pattern, which is stable and motionless.

PACS number(s): 47.20.Ky, 47.27.Te, 64.90.+b

Hexagonal patterns are an important subject of investigation in the theory of cellular structures. They are easily observed in Rayleigh-Bénard convection in non-Bussinesq fluids [1-4], in Bénard-Marangoni convection [5], autocatalytic reactions [6], etc. (see also the review [7]). However, perfect hexagonal patterns are rather difficult to observe in large aspect-ratio systems. Typically, different line or point defects emerge on the background of a hexagonal pattern. Line defects usually take the form of grain boundaries between hexagons with different orientation, or grain boundaries separating hexagons and rolls; the latter case was investigated in detail by Malomed, Nepomnyashchy, and Tribelsky [8]. Among point defects most typical are so-called "penta-hepta" defects, or pairs of cells with five and seven ridges. These defects, once having been created, are very stable (see, e.g., [3]). The purpose of the present paper is to study in numerical experiment the creation and dynamics of point defects in hexagonal patterns.

It is known that the perfect hexagon pattern is a result of the resonant interaction of three roll systems $\{\mathcal{A}_i \exp[i\mathbf{k}_i\cdot\mathbf{r}], i=1,2,3\}$ with wave vectors $\mathbf{k}_{1,2,3}$ satisfying the three-wave resonant condition $\mathbf{k}_1+\mathbf{k}_2+\mathbf{k}_3=\mathbf{0}$ (in the following we will assume that the wave numbers of all three waves correspond to the most unstable wave number $|\mathbf{k}_1|=|\mathbf{k}_2|=|\mathbf{k}_3|$ set to unity in dimensionless variables). For convection in a horizontal layer of fluid three-wave interaction appears only if the "up-down" symmetry $\mathcal{A}\to-\mathcal{A}$ of the system is broken. For example, in Rayleigh-Bénard convection this symmetry breaking is caused by temperature dependence of viscosity; in Bénard-Marangoni convection, by temperature dependence of the surface tension, etc. As a result of the nonlinear interaction systems of three rolls oriented at 120° to each other grow simultaneously, their amplitudes become equal, and the sum of their phases is zero. This process can be described by the following set of three amplitude equations for the complex amplitudes of three roll systems:

$$\partial_t \mathcal{A}_i = \epsilon\mathcal{A}_i + \alpha\mathcal{A}_j^*\mathcal{A}_k^* - (|\mathcal{A}_i|^2+\gamma|\mathcal{A}_j|^2+\gamma|\mathcal{A}_k|^2)\mathcal{A}_i, \quad \{i,j,k\}=\{1,2,3\},\{2,3,1\},\{3,1,2\}. \tag{1}$$

Here ϵ is a small supercriticality parameter, $\alpha=O(\epsilon^{1/2})$ is the coefficient of quadratic nonlinearity, describing non-Boussinesq effects, and $\gamma=O(1)$ is the ratio of the coefficient of cubic interaction of rolls of different orientation to the coefficient of cubic self-interaction. If $\alpha\neq0$ we can rescale all variables such that the new supercriticality parameter $\mu=\epsilon/\alpha^2=O(1)$, new amplitudes $A_i=\mathcal{A}_i/\alpha=O(1)$, and new $\alpha=1$,

$$\partial_t A_i = \mu A_i + A_j^* A_k^* - (|A_i|^2+\gamma|A_j|^2+\gamma|A_k|^2)A_i. \tag{2}$$

Linear stability analysis shows [9] (see also [3,10]) that if $\alpha\equiv0$ a stable hexagon pattern appears as a result of subcritical bifurcation when $-1/4(1+2\gamma)<\mu<(\gamma+2)/(\gamma-1)^2$. When the defects are present, the amplitudes of individual roll systems become functions of space as well as time. The structure of possible envelope equations was discussed by Haken [11] and Malomed, Nepomnyashchy, and Tribelsky [8], who introduced transversal diffusion terms in (1). Following them, we restrict ourselves with the most natural assumption that, besides quadratic nonlinearity, the envelopes of individual roll systems are governed by the Newell-Whitehead-Segel equations [14]

$$\partial_t A_i = \mu A_i + A_j^* A_k^* - (|A_i|^2+\gamma|A_j|^2+\gamma|A_k|^2)A_i + \hat{D}_i^2 A_i. \tag{3}$$

These differ from (2) by the linear terms $\hat{D}_i^2 A_i$ in the right-hand sides. Here $\hat{D}_i=\partial_{X_i}-i\alpha/2\partial_{Y_i}^2$, $X_i=\alpha x_i/\xi_0$, $Y_i=\alpha y_i/\xi_0$ are pairs of rescaled dimensionless Cartesian coordinates orthogonal and parallel to the rolls axes, respectively, and ξ_0 is the dimensional length scale of the system. It is important to note that in the description of hexagons we have to assume the same scaling for both x_i and y_i coordinates. Since the defects in hexagons presumably have the same characteristic size in the x and y directions, the parallel diffusion (terms proportional to $\partial_{Y_i}^2$ in $\hat{D}_i$) is usually much weaker than transversal diffusion. We keep those terms here in order to have a unified set of equations for both roll and hexagon pattern

*Permanent address: Institute of Applied Physics, Russian Academy of Sciences, 46 Ulyanov str., 603600 Nizhni Novgorod, Russia.

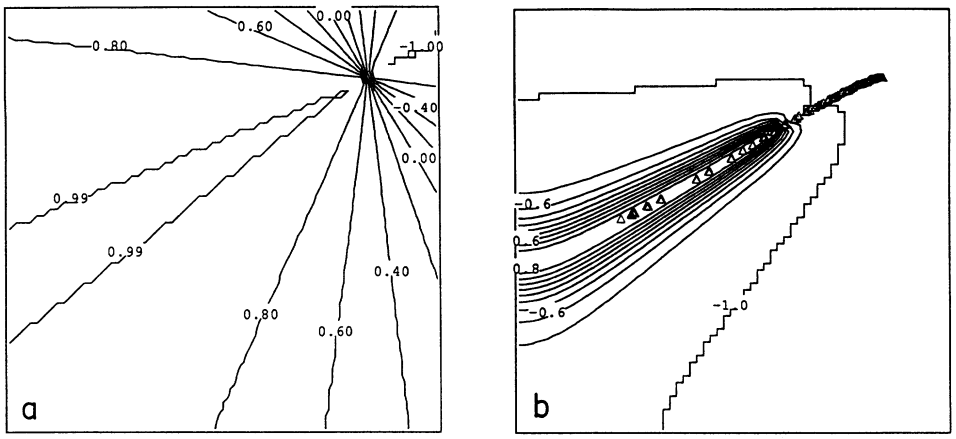

FIG. 1. (a) Profile of synchronization parameter $F=-\cos\Phi$ for one dislocation in the hexagonal pattern at $t=0$. (b) The same as in (a) for $t=10$ and the trajectory of the dislocation core (triangles, arrow shows the direction of defect motion).

formation depending on the values of parameters μ, α, and γ. Brand [12] conjectured some additional nonlinear convective terms ($\sim A\nabla A$) which may appear in the amplitude equations (3) due to a combined effect of spatial inhomogeneity and quadratic nonlinearity. We will not discuss the importance of these latter terms in detail here [13].

The set of equations (3) can be represented in a variational form

$$\partial_t A_i = -\delta\mathcal{F}/\delta a_i^*,$$

with the Lyapunov free energy functional

$$\mathcal{F}=\int dx\,dy\{-\mu(|A_1|^2+|A_2|^2+|A_3|^2)-(A_1^*A_2^*A_3^*+\text{c.c.})+\tfrac{1}{2}(|A_1|^4+|A_2|^4+|A_3|^4)$$
$$+\gamma(|A_1|^2|A_2|^2+|A_1|^2|A_3|^2+|A_2|^2|A_3|^2)+(|\hat{D}_1A_1|^2+|\hat{D}_2A_2|^2+|\hat{D}_3A_3|^2)\}, \tag{4}$$

so only static patterns can be expected as $t\to\infty$.

In our numerical simulations of Eqs. (3) we employed a pseudospectral split-step method on a square mesh with the system size 64×64 and zero-gradient boundary conditions. We used time step 0.1, mesh size 0.5, and parameters $\mu=0.5$ and $\gamma=2$. Here we will be concerned with the evolution and interaction of dislocations of individual roll systems forming a hexagon pattern.

Let us first consider as initial conditions sets of three rolls of small initial amplitude, and one of the sets contains a dislocation at some point $\{X_1^0, Y_1^0\}$. Specifically, we used the following initial conditions for the amplitudes R_i and phases ϕ_i of complex amplitudes $A_i=R_i\exp i\phi_i$:

$$R_1=R_1^0\tanh\{0.2[(X_1-X_1^0)^2+(Y_1-Y_1^0)^2]^{1/2}\},$$
$$\phi_1=\arctan[(Y_1-Y_1^0)/(X_1-X_1^0)]+\phi_0, \tag{5}$$
$$R_2=R_2^0,\quad \phi_2=0.0,\quad R_3=R_3^0,\quad \phi_3=0.0.$$

Initial amplitudes were taken small $R_1^0=0.011$, $R_{2,3}^0=0.01$ and initial phase shift $\phi_0=3\pi/2$. If there were no quadratic nonlinearity ($\alpha=0$), one of the three roll systems (since $R_1>R_{2,3}$, this is the roll set 1 with a dislocation) would suppress the other two and the dislocation itself would remain motionless since the period of rolls we take corresponds to the optimal wave number. On the contrary, within the range of parameters favoring hexagons ($\alpha=1.0$), amplitudes of all three roll sets grow, and their phases get synchronized to form hexagonal structures. However, because of the dislocation, the synchronization process is quite peculiar. In what follows, we use the parameter $F(x,y,t)=-\cos(\phi_1+\phi_2+\phi_3)$ as a measure of synchronization.

Initially, F is a smooth function of (x,y) everywhere except at the core of dislocation where it takes all values from -1 to 1 [Fig. 1(a)]. After a rather short transient ($t\simeq10.0$) $F\simeq-1$ almost everywhere but some narrow

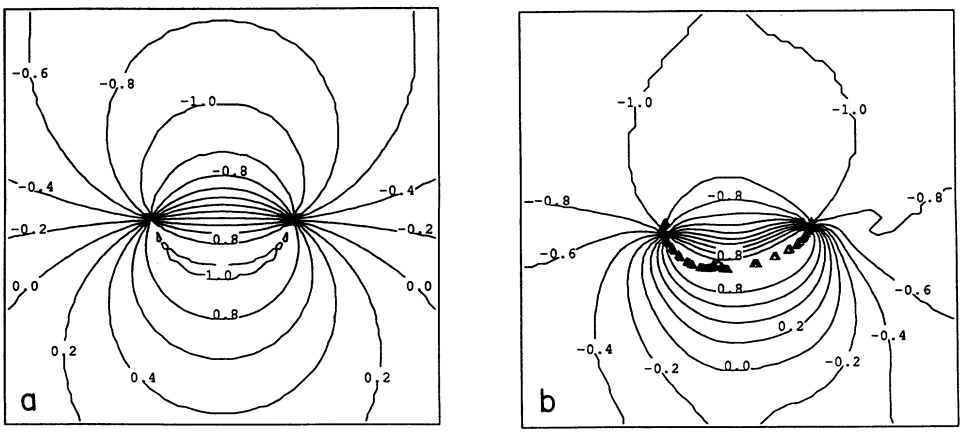

FIG. 2. (a) Profile of synchronization parameter $F=-\cos\Phi$ for two dislocations in the hexagonal pattern with $\phi_0=\pi/4$ at $t=0$. (b) The same as in (a) for $t=5$ and the trajectories of both dislocations (solid and empty triangles, arrows show the directions of defect motion).

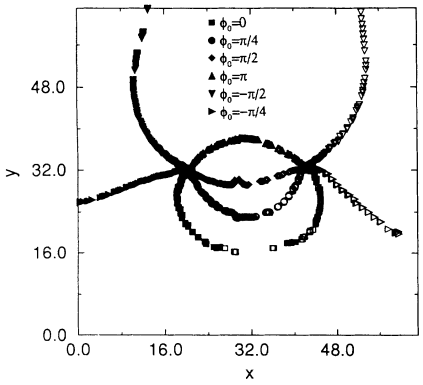

FIG. 3. Trajectories of the cores of dislocations in the hexagonal pattern for several different phase shifts between roll systems ϕ_0.

corridor starting from the core of dislocation, where it reaches the value of 1 [Fig. 1(b)]. The axis of this corridor coincides with the line $F(x,y,0)=1$. After that the dislocation starts moving quickly along this corridor [see Fig. 1(b)], and soon leaves the region of integration, and the perfect hexagon pattern with $F=-1$ everywhere eventually establishes itself.

In the second series of numerical experiments we began with two dislocations belonging to two different roll structures:

$$
\begin{aligned}
R_1 &= R_1^0 \tanh\{0.2[(X_1-X_1^0)^2+(Y_1-Y_1^0)^2]^{1/2}\},\\
\phi_1 &= \arctan[(Y_1-Y_1^0)/(X_1-X_1^0)]+\phi_0,\\
R_2 &= R_2^0 \tanh\{0.2[(X_2-X_2^0)^2+(Y_2-Y_2^0)^2]^{1/2}\},\\
\phi_2 &= -\arctan[(Y_2-Y_2^0)/(X_2-X_2^0)],\\
R_3 &= R_3^0, \quad \phi_3 = 0.0.
\end{aligned}
\tag{6}
$$

Here $\{X_1^0, Y_1^0\}$ and $\{X_2^0, Y_2^0\}$ are the coordinates of cores of dislocations, $R_{1,2,3}=0.01$, and $\phi_0=\pi/4$. Note the sign "−" in ϕ_2 which indicates different topological charges (opposite directions of phase rotation) of the two dislocations. Again, at $t=0$ the synchronization parameter changes smoothly within the range $(-1,1)$ [with the given initial phase distribution the isolines of F are circular, see Fig. 2(a)]. Now instead of a straight corridor we get a curved corridor connecting both defects [Fig. 2(b)]. After some transient period, dislocations begin to move

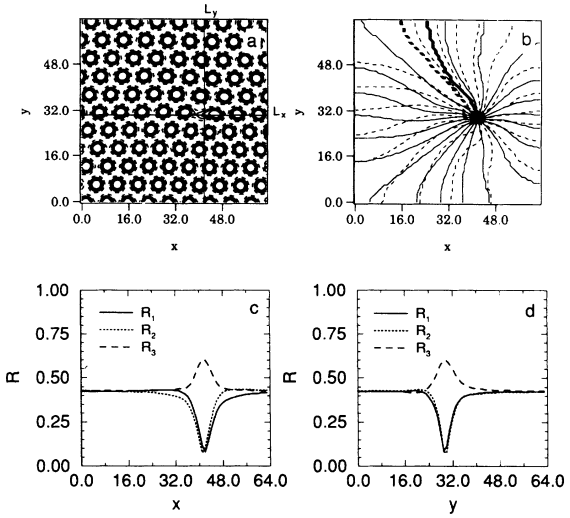

FIG. 4. "Penta-hepta" pair formed by merging of two dislocations: (a) isolines of the "temperature" field $T=\sum_{i=1}^{3} A_i \exp(ix_i)$; (b) equiphase lines of ϕ_1 (solid) and ϕ_2 (dashed); (c) cross sections of the magnitudes R_i along the line L_x in (a); (d) the same as in (c) along the line L_y in (a).

toward each other along the corridor [the trajectories are also shown in Fig. 2(b)] and eventually they stick together and form a penta-hepta defect. The trajectories of the dislocations' motion and the position of the penta-hepta pair depend strongly on the initial phase distribution. In Fig. 3 the trajectories of dislocations for several different values of ϕ_0 are shown. It is worth mentioning that the structure of the penta-hepta defect (Fig. 4) resulting from the merging of two dislocations is remarkably similar to one found in the laboratory experiment [3].

Qualitatively the behavior described above can be easily understood within the so-called *phase approximation.* First, we can assume that after initial transients all three magnitudes R_i become equal. If the spatial distribution of amplitudes is smooth, we can further assume that R_i are determined by the local phase dynamics. This approximation is valid outside cores of dislocations. The real parts of Eqs. (3) then give the equation for R:

$$\dot{R}=\mu R+\cos\Phi R^2-(1+2\gamma)R^3 \tag{7}$$

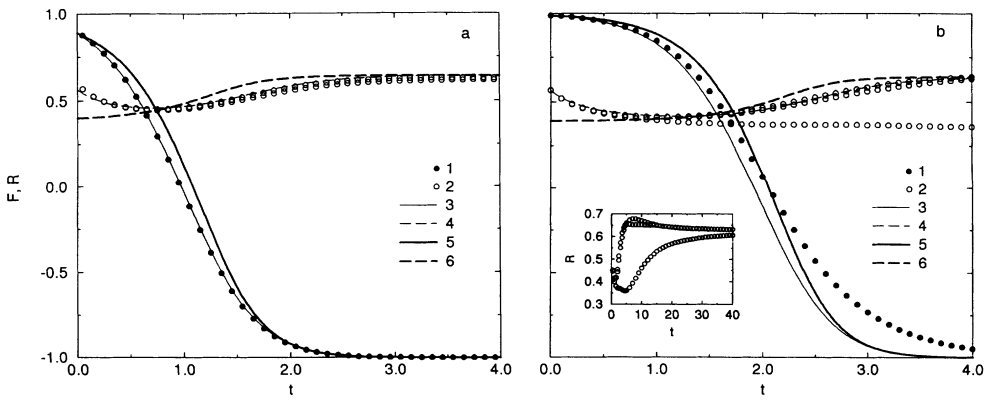

FIG. 5. Time dependence of amplitudes $R_{1,2,3}$ and synchronization parameter F in two different space locations: (a) $x=40$, $y=30$ (outside the corridor), (b) $x=40$, $y=20$ (near the axis of the corridor). Symbols 1,2 show the results of numerical simulations of F (solid circles) and all three R_i (open circles) for the full set of amplitude equations (3) with $\mu=1$, $\gamma=1.5$ and initial condition (6) with $R_{1,2,3}^0=0.65$, lines 3,4 show the corresponding solutions of the system (7),(11), and lines 5,6 show the results of the phase approximation (8),(12). The inset in (b) shows the long-term evolution of three amplitudes.

with $\Phi=\phi_1+\phi_2+\phi_3$. If the phase dynamics is slow, one can neglect the time derivative of R in (7) and arrive at the algebraic equation for R:

$$(1+2\gamma)R^2-\cos\Phi R-\mu=0. \tag{8}$$

The imaginary parts of (3) describe the phase variations

$$\begin{aligned}\partial_t\phi_1&=-R\sin\Phi+\partial^2_{x_1}\phi_1,\\ \partial_t\phi_2&=-R\sin\Phi+\partial^2_{x_2}\phi_2,\\ \partial_t\phi_3&=-R\sin\Phi+\partial^2_{x_3}\phi_3,\end{aligned} \tag{9}$$

Equations (9) with R taken from (8) also form a variational model with the Lyapunov free energy functional

$$\begin{aligned}\mathcal{F}_\phi=\int dx\,dy\Big(&-\{1/[4(1+2\gamma)]\}\{\cos\Phi[\cos\Phi+(\cos^2\Phi+B)^{1/2}]+B\ln[\cos\Phi+(\cos^2\Phi+B)^{1/2}]\}\\ &+\tfrac{1}{2}[(\partial_{x_1}\phi_1)^2+(\partial_{x_2}\phi_2)^2+(\partial_{x_3}\phi_3)^2]\Big),\end{aligned} \tag{10}$$

where $B=4\mu(1+2\gamma)$. It is easy to see now that as long as the phase variations are smooth and one can neglect space derivatives in (10), the density of the Lyapunov functional is a monotonous function of the parameter F. Within the same assumptions the equation for Φ is simply

$$\dot\Phi=-3R\sin\Phi, \tag{11}$$

or after substitution of R from (8),

$$\dot\Phi=-\{3/[2(1+2\gamma)]\}[\cos\Phi+(\cos^2\Phi+B)^{1/2}]\sin\Phi, \tag{12}$$

so Φ goes to 0 ($F\to-1$) everywhere except on the lines where $\Phi=\pi(F=1)$, and thus corridors of large F are formed. The only points where these lines can originate and/or end (except infinity) are the dislocations. Therefore the dislocations start to move (due to a Peach-Köhler-type force, see [15]) as to decrease optimally the free energy of the system, i.e., along the lines of maximum $F=1$ and either go to infinity or meet each other and stick, thus creating a "penta-hepta" pair.

To test the validity of the phase approximation we simulated the temporal dynamics of the synchronization parameter F and magnitudes of the rolls R_1,R_2,R_3 in some fixed space locations using the full set of amplitude equations (3), simplified system of equations (7),(11), and phase approximation model (8),(12). We used a one-dislocation initial condition (6) and parameters $\mu=1$, $\gamma=1.5$. In Fig. 5 we present the results of the simulations at two different locations: outside the corridor (a), and within the corridor (b). As one can see, for the off-corridor location system (7),(11) provides a very good description, but the pure phase approximation [Eqs. (8),(12)] leads to certain errors which are due to nonadiabaticity at the initial stage of the phase synchronization. For the in-corridor location both simplified descriptions are rather inaccurate. The reason for this is quite simple. Indeed, since in accordance with (12) the corridors get more and more narrow, eventually the assumption of smoothness of phase dynamics is violated in their vicinities and the diffusion terms in (9) (and also in the equations for R_i) become important. In the long run some stationary profile of corridors is established due to phase diffusion (these stationary corridors are analogous to the kink solutions of the sine-Gordon equation). That is why the above arguments hold only qualitatively. Nevertheless, they explain correctly the main features of behavior of individual roll dislocations and the penta-hepta pair formation.

The details on the dislocation motion as well as many other interesting aspects of the spatiotemporal dynamics of the hexagonal patterns are still left beyond the framework of the present paper. They include, for example, the interaction (and annihilation) of dislocations of the same roll system, interaction of penta-hepta pairs, Eckhaus instability of hexagons, dynamics of the line defects in hexagonal patterns, nonvariational effects, etc. We plan to address these issues in future publications.

The authors thank H. Abarbanel and E. Bodenschatz for reading an early version of the paper and many useful comments. This work was supported partially by the U.S. Department of Energy under Contract No. DE-FG03-90ER14138 and partially by the Office of Naval Research under Contract No. N00014-D-0142 DO#15. M.I.R. thanks the Institute for Nonlinear Science, University of California, San Diego for warm hospitality.

[1] R. W. Walden and G. Ahlers, J. Fluid. Mech. **109**, 89 (1981).
[2] S. Ciliberto *et al.*, Phys. Rev. Lett. **61**, 1198 (1988).
[3] S. Ciliberto *et al.*, Phys. Rev. Lett. **65**, 2370 (1990).
[4] E. Bodenschatz *et al.*, Phys. Rev. Lett. **67**, 3078 (1991).
[5] P. Cerisier *et al.*, Phys. Rev. A **35**, 1949 (1987).
[6] Q. Ouyang and H. L. Swinney, Nature (London) **352**, 610 (1991).
[7] M. Cross and P. Hohenberg, Rev. Mod. Phys. **65**, 851 (1993).
[8] B. A. Malomed *et al.*, Phys. Rev. A **42**, 7244 (1990).
[9] F. H. Busse, J. Fluid Mech. **30**, 626 (1967).
[10] B. A. Malomed and M. I. Tribelky, Zh. Eksp. Teor. Fiz. **92**, 539 (1987) [Sov. Phys. JETP **65**, 305 (1987)].
[11] H. Haken, *Advanced Synergetics* (Springer, New York, 1983).
[12] H. R. Brand, Progr. Theor. Phys. Suppl. **99**, 442 (1989).
[13] Scaling considerations show that for balancing all the terms in the envelope equation the dimensional coefficient of quadratic nonlinearity has to be of the order of $\epsilon^{1/2}$, and with this scaling nonlinear terms $\sim A\nabla A$ are of the higher order than linear diffusion terms. However, since these terms destroy the variational nature of Eqs. (3) they can be important for the long-term behavior of the system.
[14] A. C. Newell and J. A. Whitehead, J. Fluid Mech. **38**, 279 (1969); L. A. Segel, *ibid.* **38**, 203 (1969).
[15] E. D. Siggia and A. Zippelius, Phys. Rev. A **24**, 1036 (1981).